ELSEVIER

Journal of Neuroscience Methods 63 (1995) 85–92

JOURNAL OF NEUROSCIENCE METHODS

Microminiature molding techniques for cochlear electrode arrays

G.E. Loeb [a,*], R.A. Peck [a], D.W. Smith [b]

[a] *Bio-Medical Engineering Unit, Queen's University, Kingston, Ont. K7L 3N6, Canada*
[b] *Department of Otolaryngology, Head and Neck Surgery, Duke University Medical Center, Durham, NC, USA*

Received 21 October 1994; revised 23 May 1995; accepted 31 May 1995

Abstract

We provide a general method for producing a variety of small, complex electrode arrays based on injection molds produced using computer-aided drafting and machining (CAD–CAM) procedures and a novel method for connecting to the very fine electrical leads associated with the individual contacts of such arrays. Cat-sized cochlear electrode arrays with up to eight contacts were built according to these methods and their electrical contacts were characterized in vitro by impedance spectroscopy and in vivo by monitoring impedance for over 1 year of intermittent stimulation in chronically instrumented animals.

Keywords: Cochlear prosthesis; CAD-CAM; Silicone rubber

1. Introduction

In biomedical research, it is often desirable to produce small, complexly shaped composite structures from biocompatible materials for chronic interfacing with living tissues. One such application that has important clinical and economic impact is cochlear prosthetics to restore hearing in cases of primary sensorineural deafness due to loss or malfunction of the hair cells that transduce acoustic vibrations into neuroelectric activity (for review, see Loeb, 1990). Multicontact electrodes are threaded into the scala tympani of the inner ear where they are used for electrical stimulation of the spiral ganglion cells comprising the auditory nerve. The geometrical relationship between electrode contacts and neurons is a critical variable in obtaining selective, regional control of the tonotopically mapped neural signals (Rosen, 1990). The mechanical properties of the electrode array are critical for the successful insertion and fixation of the electrodes in this delicate and difficult to access part of the body. Animal and clinical research requires efficient and reliable production of a wide range of complex electrodes with precisely controlled and reproducible electrical and mechanical handling properties.

Several approaches to the fabrication of specific electrode geometries have been described (Loeb et al., 1983; Chouard et al., 1985; Shepherd et al., 1985; Fedorova et al., 1988; Xue and Pfingst, 1989; Pulec et al., 1989; Van der Puije et al., 1989) or can be inferred from an examination of commercial cochlear electrodes. We present a more general method based on computer-aided design and machining (CAD-CAM) that facilitates the rapid design and efficient fabrication of a wide range of cochlear electrodes for experimental use. This method is particularly suited to animal research in which precise electrode geometries must be achieved in unusually small cochleas. We also present a novel technique for the solderless attachment of fine wires to conventional solder pots on subminiature connectors suitable for percutaneous use in small animals.

2. Requirements

2.1. Geometry

The stimulating current must pass from metal leads into the aqueous body fluids through the metal-electrolyte interface of the individual electrode contacts. The ability to do so without inducing damaging, irreversible electrochemical reactions depends on the nature, surface area and condition of the exposed metal surface (for review, see Loeb et al., 1982). Thus, one critical requirement is for a clean and reproducible demarcation of the exposure of each contact.

* Corresponding author: Abramsky Hall, Queen's University, Kingston, Ont. K7L 3N6, Canada. Tel.: (613) 545-2790; Fax: (613) 545-6802; E-mail: LOEB@BIOMED.QUEENSU.CA.

Elsevier Science B.V.
SSDI 0165-0270(95)00091-7

Electrical currents must be injected through a pair of electrodes acting alternatively as source and sink for biphasic stimulation waveforms. The exact spacing and orientation of the resultant dipole source with respect to the neural processes to be stimulated is a strong determinant of which neurons are actually recruited (Ranck Jr., 1975; Eddington et al., 1978; Merzenich et al., 1979). Thus, the fabrication methods must permit accurate and reproducible positioning of contacts anywhere on the surface of the composite electrode array.

2.2. Placement

As shown in Fig. 1F, the neuronal cell bodies comprising the spiral ganglion are clustered within the bony medial wall of the scala tympani over the extent of its spiral course. Their axons project ventrally and centrally toward the axial core of the spiral where they form the auditory nerve. Their apical dendrites project laterally toward the organ of Corti, coursing laterally (radially to the cochlear spiral) through the bony partition between scale tympani and scala media and entering the basilar membrane through the habenula perforata. The dendrites and the cell body are myelinated and probably electrically excitable, but the presence and condition of the dendrites is quite variable depending on the etiology of deafness (Hinojosa, 1990). One useful way to describe the circumferential position of the spiral ganglion is in terms of a clockface centered in the scala tympani. For the mid-basal turn of the cat cochlea that was targeted in these studies, the spiral ganglion tends to be located around 02:00 h and the habenula perforata around 12:00 h.

The resistivity of the fluid-filled cochlear chambers is probably close to that of isotonic mammalian saline (65 Ω/cm) while the resistivity of the bony wall surrounding the neurons is probably an order of magnitude higher (Finley, 1989). The tendency for electrical currents from the stimulating electrodes to pass parallel to and thus depolarize the radially deployed neurons depends critically on the exact positioning of the source and sink with respect to portals such as the habenula perforata and the impediment to current flow in the scala that is caused by the electrode array itself (Finley, 1989).

Premolded curvature to follow the cochlear spiral may be useful in keeping the contacts close to the medial wall and reducing any tendency to apply force to the fragile basilar membrane during insertion, but the array must then withstand any mechanical straightening required to initiate insertion. As described previously for the human cochlea (Loeb et al., 1983), this requires gathering of the inelastic wire leads into an axially central bundle or 'rib' within the elastomer that forms the body of the array. The cat cochlear arrays described here make only a quarter turn just past the initially straight and rapidly narrowing basal segment (see Figs. 2 and 3), so they can be inserted with little deformation of the molded curved shape.

The electrode array must be inserted blindly through the small entry afforded by making a cochleostomy at the round window. Thus, the cross-sectional shape and size of the electrode array largely determines how it and its various contacts will lay in the scala tympani. It is often desirable to have molded features such as tabs to help the surgeon orient the electrode array and judge insertion depth and to provide anchoring sites for surgical fixation with sutures or adhesives (Fig. 1A,C).

2.3. Biocompatibility

Obviously the electrode array needs to be fabricated entirely from materials that will withstand prolonged immersion in body fluids and that will not release toxic compounds into those fluids (Loeb et al., 1982; Burgio, 1986). In the case of the electrode leads and contacts, this means selection of a metal that can be operated safely at high charge densities at the metal–electrolyte interface and avoidance of junctions between dissimilar metals that may result in galvanic corrosion. The lead wires must be individually insulated to avoid shorting to each other in the mold or becoming bridged by fluid that tends to accumulate in any voids within the body of the electrode and the multilead cable to a connection point. The body of the electrode needs to be a pliable elastomeric material that induces a minimal foreign body reaction and that maintains mechanical and dielectric integrity indefinitely in vivo.

3. Materials and methods

In keeping with most previous researchers, we have selected the noble metal alloy of 90% platinum–10% iridium (Pt–Ir) for the electrode leads and contacts (37 μm diameter, California Fine Wire). The 10% iridium alloy increases the tensile strength of the normally ductile pure platinum; higher iridium content produces excessive springiness of the leads, interfering with molding and handling the array. The ends of the wires were melted into balls with sufficient surface area to support reversible charge transfer over the required functional range. For example, a cleanly exposed contact 0.15 mm in diameter (see Fig. 1C) has a geometric surface area of 1.8×10^{-4} cm^2 (assuming no surface roughening), which would support a stimulus charge-per-phase of 54 nC at a proposed electrochemical limit of about 300 μC/cm^2 (Brummer et al., 1983). The actual behavioral thresholds obtained with these electrodes were generally 1–20 nC for biphasic pulses with phase durations of 0.1–10 ms (Smith et al., 1995).

We have had extensive experience with various dielectric coatings that can be obtained commercially on fine wires and have settled on a multilayer Teflon FEP coating (Phoenix Wire, South Hero, VT). This material is mechan-

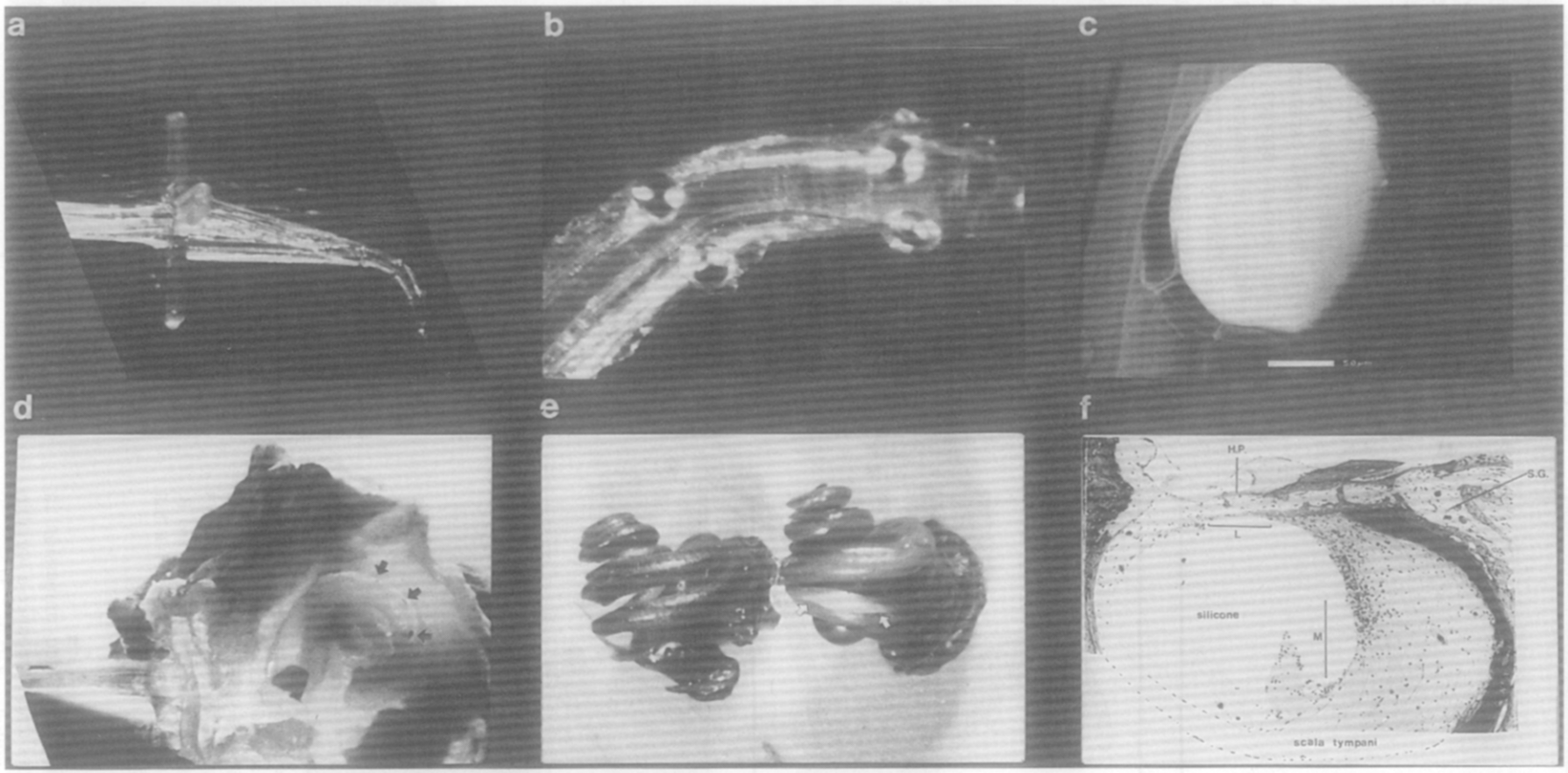

Fig. 1. A: cochlear electrode for cat cochlea with 8 contacts (3 radial bipolar pairs plus basal and apical monopolar sites) and fixation tabs at round-window entry point. B: detail of bipolar contact region. C: scanning electron micrograph of 1 Pt–Ir contact showing cleanly demarcated exposure through window in the silicone rubber carrier. D: test insertion of electrode array into cadaver temporal bone, showing correct alignment of 3 lateral contacts (small arrows) under medial edge of translucent basilar membrane. E: castings of cat cochlear scalae for dimensioning (left) and identification of bearing points of test silicone electrode form (right, arrows) inserted into cadaver temporal bone before injection of casting compound. F: radial cross-section through the basal turn of a cat cochlea implanted for 10 months with cochlear electrode array (removed prior to sectioning; position of bulges in surrounding scar tissue denote medial (M) and lateral (L) contacts) with respect to habenula perforata (h.p.) and spiral ganglion (s.g., very sparse cell survival after deafening by intracochlear injection of neomycin).

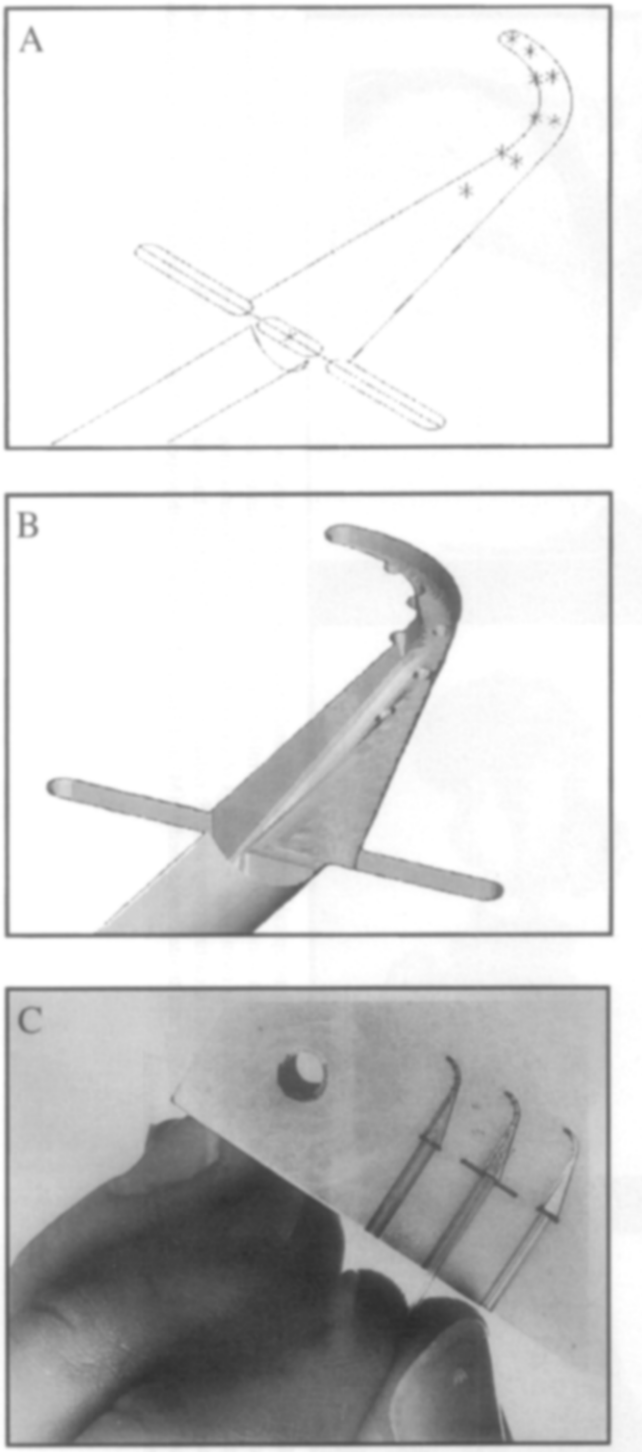

Fig. 2. A: MASTERCAM tool contours required to define the 8-contact cochlear electrode with surgical fixation tabs shown completed in Fig. 1A,B. 3-D shaded rendering of simulated mold to be cut by the NC-mill commands generated by MASTERCAM. C: completed mold block with 3 mold cavities; center cavity machined according to design A and B, shown being loaded with silicone tube containing a set of Pt–Ir ball electrodes and leads at the beginning of the molding process.

ically tough and stable during prolonged immersion in saline. The coating process does tend to produce a variable but low rate of minute pinhole defects. However, impedance testing of insulated wire loops indicates that these pinholes, even when present, represent a negligible leakage path compared to the conductance of the exposed electrode contact and that this path does not enlarge with prolonged soaking and stimulation. In any event, most of the length of each wire will be securely encased in the silicone rubber, making the probability of bridging between apposed pinholes in adjacent wires extremely low. By contrast, polyimide coatings are often defect free initially but tend to deteriorate exponentially with prolonged immersion. This problem appears to be related to the synergistic effects of mechanical stress plus hydrolysis because there is relatively little deterioration in unstressed, soaked wires or stressed, dry wires. Where such wires traverse together across small voids in the silicone rubber (which occurs commonly in the extended length of the cable from the electrode array itself to an external connector), interlead impedances may deteriorate from unmeasureably large to a few kilohms in weeks to months in vivo.

The body of the electrode is molded from medical grade silicone rubber elastomer (Dow Corning Silastic MDX-4-4210). This is a platinum-catalyzed polymer that can be rapidly and fully heat-cured and that contains essentially no leachable impurities. Like all silicone elastomers, it tends to flow well into complex mold geometries under combined vacuum and pressure injection at room temperature.

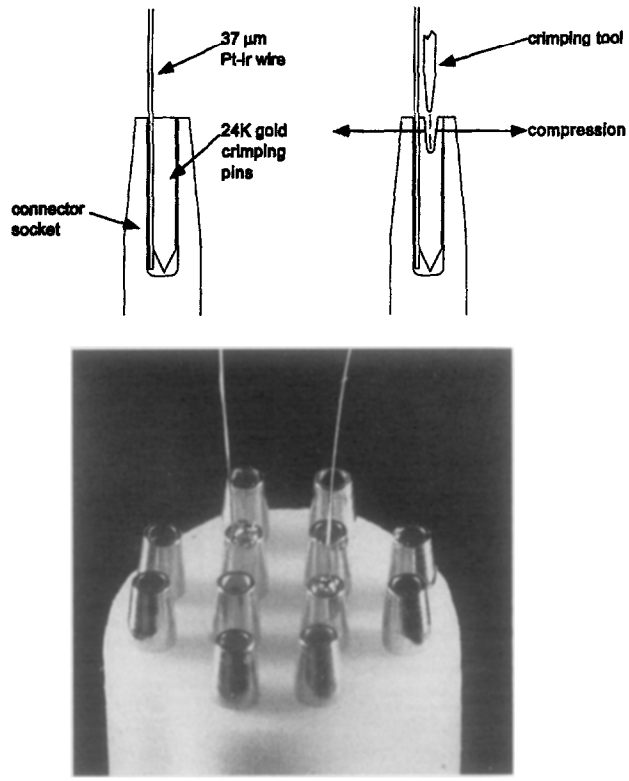

Fig. 3. Top shows schematic process for 'reverse-crimp' termination of fine Pt–Ir wires into gold-plated solder pots of multipin Microdot connector insert used in chronic skull pedestal connector as shown at bottom.

3.1. Mold design and fabrication

The detailed shape and dimensions of the electrodes were determined by examining cadaver temporal bone dissections in which the intended site of the electrode in the scala tympani can be viewed from above by looking through the translucent basilar membrane (Fig. 1D). These were supplemented by histological cross-sections perpendicular to the cochlear chambers taken at various measured depths from the round window (see also Loeb et al., 1983; Walby, 1985). These cross-sections were used to determine the maximal dimensions of a particular electrode profile that could be accommodated at each depth and to anticipate the orientation and bearing points on the walls of the scala tympani when the electrode was inserted to the depth at which resistance was felt. These bearing points were confirmed by inserting trial electrodes into the scala tympani of a cadaver temporal bone followed by injection and curing of a polymer throughout the scalae and subsequent removal of the surrounding tissues to leave the casts shown in Fig. 1E. The cross-sections were also used to select the desired radial location of electrode contacts on the surface of the electrode form vis-a-vis the cell bodies and processes of the spiral ganglion cells.

At these fine dimensions, the exact profile that can be obtained depends on the size and profile of the cutting tool that will be used and the sophistication of the numerically controlled milling machine that will generate the tool path. One important consideration is whether the profile can be flat on one side, which permits use of a single-sided mold with a flat cover, as opposed to requiring a 2-sided mold whose halves must be precisely aligned during the injection process. Thus, the design emerges from iterative interactions and compromises between the experimentalist and the machinist.

CAD-CAM mold design usually proceeds by converting a 3-dimensional (3-D) drawing of the desired mold contours into a set of tool paths for milling out the desired cavity using one or more stock cutters. For the very small, curved molds required in this application, we found it more convenient to consider the shape and size of the available cutting and drilling tools and to define tool paths that would leave the desired shape (Fig. 2A). This is easily done with the drawing package contained within the MASTERCAM software package (CNC Software, Tolland, CT) that we used to generate the lengthy string of commands required for our Dynamite 2400 NC-milling machine to follow those tool paths. The MASTERCAM software includes a simulation package (called MTV) which produces an animation of the milling process and a 3-D shaded rendering of the mold cavity that will be left after its completion (Fig. 2B). These are very useful to confirm that the tools will not collide with the work piece and that the final shape will be as envisioned.

In addition to the milled-out profile of the cochlear electrode array (Fig. 2C), the finished mold includes small depressions in the walls where the electrode contacts will be affixed. These are typically made with a 175 μm diameter drill using the NC-mill to produce the precise depth in the block before milling the mold profile; this allows shallow depressions (typically 50 μm deep) to be made tangential to the mold side-walls without the drill 'walking'. Drill holes are also placed for fill and exhaust ports at the apical and basal ends of the electrode array, respectively. As shown in Fig. 1A,B, it is often desirable to mold tab-shaped projections at the base of the electrode array to provide anchoring points for fixation just outside the round window. A wide, shallow groove is placed in the mold surface from the edge of the block to the beginning of the electrode array. This groove accommodates the silicone rubber tubing housing the leads so that it is incorporated into the molded electrode assembly (shown being positioned into the mold in Fig. 2C).

3.2. Leads and contacts

Spherical electrode contacts were formed on the ends of the insulated lead wires by melting a measured length (e.g., 2.5 mm for 250 μm diameter ball) of the lead in a microtorch flame, taking care to protect the region of the lead immediately behind the molten ball by holding it in relatively large forceps that acted as a heat sink. The back ends of the desired number of leads are threaded through commercial silicone rubber tubing (Dow Corning Silastic 602-135, 0.020″ ID × 0.037″ OD), leaving the ball contacts protruding by about 1 cm.

3.3. Molding process

The aluminum mold is cleaned with medical detergent, rinsed in distilled water, and blown dry with compressed air. A thin coating of 20% polyvinyl alcohol (PVA) is applied with an artists brush over the entire mold surface, including the fill and exhaust ports, and air-dried at 65°C (the ports may require opening with a fine wire probe). The PVA coating in the depressions where the balls will be located is particularly important because this covers and protects the contact surface of the ball so that it is not covered by silicone rubber when the mold is filled. The bottom mold block is placed on a hotplate to maintain it at 65°C, the temperature at which the silicone elastomer cures on contact. The tube containing the leads is placed in the entry groove and held down with a weight. Each ball contact is pulled out from the end of the tube and placed in the desired contact depression, usually working from basal to apical. The ball is held in place with a hollow probe (made from a blunt piece of hypodermic tubing whose inside diameter is smaller than the ball diameter) and small dabs of the silicone elastomer are applied around it (using a Portionaire PV-200-VP pneumatic dispenser), where they cure to anchor it. Similar dabs can be used to anchor the individual leads and the carrier tubing in desired positions within the mold.

After all of the electrode contacts are in place, the mold halves are bolted together and placed in a vacuum chamber where the injection port is attached to a feedthrough from a pressure injection system. The chamber and the air space above the elastomer in the injection system are pumped down simultaneously to avoid extruding the elastomer prematurely. After 45 min of vacuum, the elastomer is injected into the mold at 80 psi until the exhaust port shows a flow of elastomer with no bubbles. The chamber and the elastomer are vented to room pressure and cured overnight at room temperature (curing at higher temperatures may release dissolved air as bubbles in the elastomer). The mold is soaked and opened under running hot water, which dissolves the PVA release agent. The completed electrode assembly is removed from the mold after cutting free the sprues at the injection and exhaust ports. It is examined under a dissecting microscope and any small amounts of cured elastomer that form a 'flash' in the seams between the mold halves or over the contacts are removed with fine forceps.

3.4. Termination of leads

We developed a novel method for the simultaneous electrical and mechanical attachment of fine wires to typical gold-plated solder pot terminals found on the pins of subminiature connectors (e.g., Microtech FP-12S-1, suitable for skull pedestals, or GF-8, suitable for percutaneous cables). Soldering is often difficult on very fine wires and tends to leave flux residues that interfere with encapsulation over the solder joint. Even cleaned and well-encapsulated solder is undesirable when the connector will be exposed to body fluids or high humidity because water vapor diffusing through polymeric encapsulants tends to condense and set up galvanic corrosion on the solder surface. Conventional crimp connections to these very fine, relatively brittle wires are difficult to achieve reliably without weakening the wire, particularly in high density connectors with restricted access to the pins. The reverse-crimp technique (Fig. 3) requires only a short length of soft gold wire somewhat smaller than the inside diameter of the solder pot. The gold slug is inserted alongside the bare wire in the solder pot and deformed laterally by pushing a sharp dental pick into its top end. This compresses the wire against the side wall of the solder pot, making a mechanically tight connection without significantly deforming the harder Pt–Ir wire. In essence, this technique reverses the usual relationships of a typical crimp connection, in which a hard material is compressed onto a relatively malleable wire; hence, we call this a 'reverse-crimp connection.'

3.5. Characterization

After removal from the mold and microscopic inspection for any visible defects, the electrode contacts are cleaned by immersing in saline and subjecting to −9 VDC (vs. a platinum foil indifferent electrode) for a few seconds to produce electrolysis bubbles that scrub the metal surface of each contact, removing any oils or oxides that may have accumulated during handling. Observing the streams of bubbles also provides an easy way to identify which lead is attached to which contact to facilitate correct wiring to the connector. The electrode is removed from the saline bath and reimmersed to remove gas air bubbles that may be trapped around the contacts. Impedance is measured for each contact with respect to the indifferent electrode using a 100 nA, 1 kHz sine wave (Bak Electronics IMP-1 impedance tester). More complete information about the condition of the contacts and the compliance voltage required to generate various waveforms of stimulus current was also obtained by impedance spectroscopy (Voltech T2400) as shown in Fig. 4.

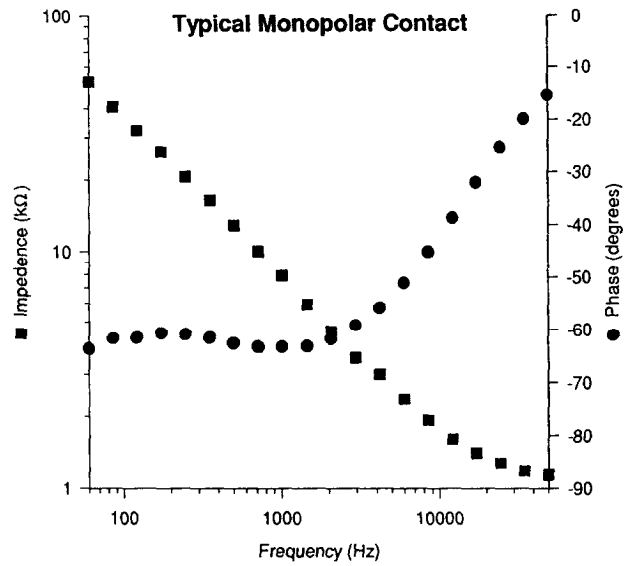

Fig. 4. Impedance spectroscopy showing magnitude (■, left abscissa) and phase angle (●, right abscissa) of 1 contact of a cochlear electrode array vs. a large indifferent electrode in normal saline, for 20 frequencies of sinusoidal stimulation (±0.1 V) distributed at log steps from 60 Hz to 50 kHz.

4. Results

4.1. Impedance

For a series of 10 electrode arrays having different geometrical arrangements of similarly sized contacts, the monopolar impedance values ranged from 8 to 30 kΩ during the initial testing in saline at 1 kHz. The impedance of bipolar pairs was only slightly less than the sum of the two monopolar impedances, suggesting that most of this impedance arises from the metal–electrolyte junction rather than the intervening fluid. This is consistent with the impedance spectroscopy in Fig. 4, which shows a predomi-

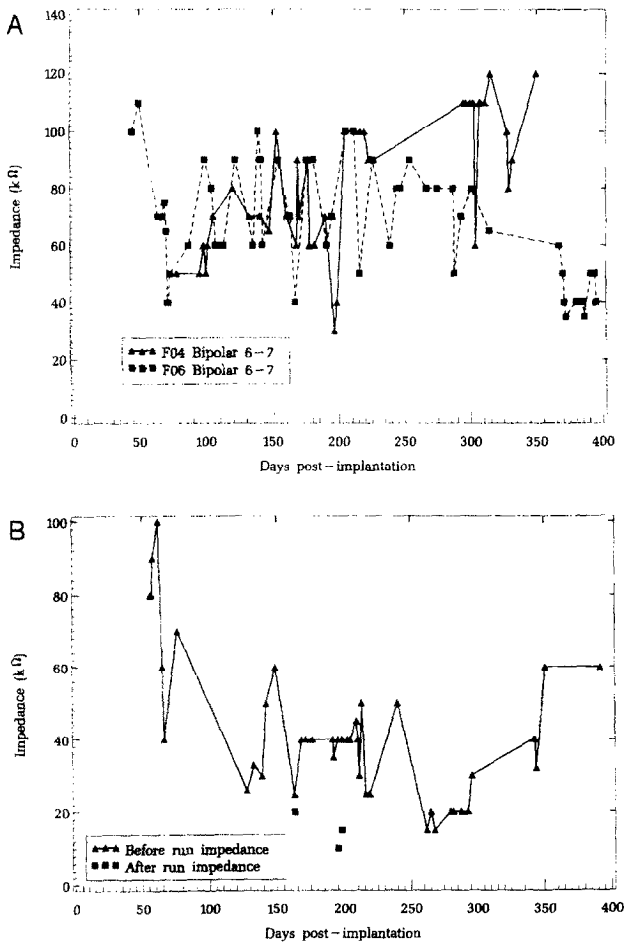

Fig. 5. Impedance (for 0.1 μA, 1 kHz sinusoid) vs. time. A: same basal bipolar pair in each of 2 cochlear electrode arrays implanted chronically in neomycin-deafened cats (F04 and F06) and stimulated at irregular intervals at levels above behavioral threshold for discrimination task. B: monopolar impedances from an infrequently stimulated apical contact in animal F04 with 3 impedance values (■) obtained after behavioral trials in which the contact was stimulated.

nantly capacitive interface at frequencies below 10 kHz. Post-operative impedances were somewhat higher and more variable, depending on the exact placement of the contact against the side walls of the scala tympani and any encapsulation by connective tissue. Bipolar pairs generally ranged from 30 to 120 kΩ (Fig. 5A). It was common for impedance values to drift substantially higher in electrodes that had not been stimulated electrically for extended periods of time, returning to more typical values after a few seconds of stimulation at typical levels for cochlear prostheses (e.g. 100 μA, 1 kHz sinusoid). Most of the cyclical fluctuations shown in Fig. 5A were due to this effect, which can be seen more clearly in Fig. 5B, which shows a few impedance values measured before and after behavioral experiments in which a variety of sinusoidal stimuli were employed. Presumably these reversible increases in impedance were due to accumulation of thin layers of poorly conductive coatings such as proteins that spontaneously denature on the platinum surface due toits catalytic action. Given the irregular schedule of impedance measurement and electrical stimulation employed in these experiments, these data serve mainly to demonstrate that these electrodes tend to be sufficiently stable over time for their intended purpose.

4.2. Placement

Fig. 1D shows the electrode inserted into a cadaver cat temporal bone that has been ground away to permit the first turn of the scala tympani to be visualized through the translucent basilar membrane. The lateral contacts are just visible in correct alignment with the edge of the basilar membrane, near the habenula perforata. Fig. 1F shows a cross-section of the cochlea after such an electrode had been in place for about 10 months. The electrode was removed prior to sectioning but the scar tissue around it shows the alignment with respect to the walls of the scala tympani and the spiral ganglion cells.

4.3. Reliability

Several different designs of cat cochlear electrode arrays with 8–11 contacts have been produced using these techniques and used successfully in various acute and chronic neurophysiological and behavioral experiments. Yields of satisfactory electrodes are generally 60–80%, depending on operator experience and dexterity. Defects are readily visible under a dissecting microscope (e.g., air bubbles, displaced contacts, etc.). Electrodes that pass such scrutiny have highly reproducible dimensions that correspond within 25 μm to the design and simulated molds.

The longest periods of implantation have been over 1 year. Since switching from polyimide to Teflon insulation on the wires, the only limiting factors have been wear or damage to the percutaneous connectors rather than degradation of the electrodes. Details of behavioral and electrophysiological (EABR) responses obtained chronically with these electrodes in four animals are reported in Smith et al., 1994, 1995.

5. Discussion

Most of the progress in cochlear prostheses over the past decade has come from improvements in the speech processors and stimulation strategies (Wilson et al., 1991) rather than in electrode designs. This is not because any particular standard or optimal electrode array has been identified; on the contrary, clinical arrays have diverse designs, many of which are difficult to reconcile with biophysical theories of electrical stimulation. The limiting factor in exploring new electrode designs has been largely their difficulty of manufacture and the comparison of function across subjects, as opposed to the relative ease of writing new algorithms and software for speech processing

and stimulus specification and comparing results within subjects.

Inevitably, a point of diminishing returns seems likely to be reached, in which further improvements of speech processors cannot be appreciated without accompanying improvements in the numbers and selectivity of the stimulation channels defined by the electrode geometry. We hope that this presentation will make the development of novel cochlear electrode arrays more accessible for researchers. We note that numerically controlled milling machines (NC-mills) with sufficient precision are now commonly available in workshops on university campuses and at local small machining contractors. The equipment costs less than US$20 000 and academic versions of suitable, easily learned CAD-CAM software packages for PC-standard computers are often available for under $3000.

Acknowledgements

This research was supported by NIH Program-Project Grant P01-DC-00036. The authors thank Dr. Pat Leake of the University of California at San Francisco for the histological sections and Mr. Chuck Byers of the Alfred E. Mann Foundation for Scientific Research for much helpful advice on CAD-CAM processes, micromachining and electrode fabrication. The wire attachment technique is the subject of US Patent #5,430,254.

References

Brummer, S.B., Robblee, L.S. and Hambrecht, F.T. (1983) Criteria for selecting electrodes for electrical stimulation: theoretical and practical considerations, Ann. NY Acad. Sci., 405: 159–171.

Burgio, P. (1986) Safety considerations of cochlear implantation, Otolaryngol. Clin. N. Am., 19: 237–247.

Chouard, C.H., Fugain, C. and Meyer, B. (1985) Technique and indications for the French multichannel cochlear implant 'Chorimac-12' for total deafness rehabilitation, Am. J. Otol., 6: 291–294.

Eddington, D.K., Dobelle, W.H., Brackmann, D.E., Mladejovsky, M.G. and Parkin, J.L. (1978) Auditory prostheses research with multiple channel intracochlear stimulation in man, Ann. Otol. Rinol. Laryngol., 87: 1–39.

Fedorova, V.N., Remizov, A.N., Bogomil'skii, M.R. and Gontsov, L.D. (1988) Electrodes for cochlear implantation. [Russian], Vestnik. Oto-Rhino-Laringologii., 50–52.

Finley, C.C. (1989) A finite element model of radial bipolar field patterns in the electrically stimulated cochlea: two- and three-dimensional approximations and tissue parameter sensitivities, IEEE 11th Annu. Conf. of the Eng. Med. Biol. Soc.

Hinojosa, M.D. (1990) Pathology of profound sensorineural deafness, Ann. NY Acad. Sci., 98: 211–220.

Loeb, G.E. (1990) Cochlear prosthetics, Ann. Rev. Neurosci., 13: 357–371.

Loeb, G.E., Byers, C.L., Rebscher, S.J., Casey, D.E., Fong, M.M., Schindler, R.A., Gray, R.F. and Merzenich, M.M. (1983) The design and fabrication of an experimental cochlear prosthesis, Med. Biol. Eng. Comput., 21: 241–254.

Loeb, G.E., McHardy, J. and Kelliher, E.M. (1982) Neural prosthesis. In: D.F. Williams (Ed.), Biocompatibility in Clinical Practice, Vol. II, CRC Press, Boca Raton, FL, pp. 123–149.

Merzenich, M.M., White, M., Vivion, M.C., Leake-Jones, P.A. and Walsh, S.M. (1979) Some considerations of multi-channel electrical stimulation auditory nerve in the profoundly deaf: interfacing electrode arrays with the auditory nerve array, Acta Oto. Laryngol., 87: 196–203.

Pulec, J.L., Smith, J.C., Lewis, M.L. and Hortmann, G. (1989) Multichannel extracochlear implant, Am. J. Otol., 10: 84–90.

Ranck, J.B. Jr. (1975) Which elements are excited in electrical stimulation of mammalian central nervous system: a review, Brain Res., 98: 417–440.

Rosen, S. (1990) Electrode placements for cochlear implants: a review. Br. J. Audiol., 24: 411–418.

Shepherd, R.K., Clark, G.M., Pyman, B.C. and Webb, R.L. (1985) Banded intracochlear electrode array: evaluation of insertion trauma in human temporal bones, Ann. Otol. Rhinol. Laryngol., 94: 55–59.

Smith, D.W., Finley, C.C., van den Honert, C., Olszyk, V.B. and Konrad, K.E.M. (1994) Behavioral and electrophysiological responses to electrical stimulation in the cat. I. Absolute thresholds, Hear. Res., 81: 1–10.

Smith, D.W., Watt, S., Konrad, K.E.M. and Olszyk, V.B. (1995) Behavioral auditory thresholds for sinusoidal electrical stimuli in the cat, J. Acoust. Soc. Am., in press.

Van der Puije, P.D., Pon, C.R. and Robillard, H. (1989) Cylindrical cochlear electrode array for use in humans, Ann. Otol. Rhinol. Laryngol., 98: 466–471.

Walby, A.P. (1985) Scala tympani measurement, Ann. Otol. Rhinol. Laryngol., 94: 393–397.

Wilson, B., Finley, C., Lawson, D., Wolford, R., Eddington, D. and Rabinowitz, W. (1991) Better speech recognition with cochlear implants, Nature, 352: 236–238.

Xue, X.L. and Pfingst, B.E. (1989) Inner ear implants for experimental electrical stimulation of auditory nerve arrays, J. Neurosci. Methods, 28: 189–196.